IOP Conference Series: Materials Science and Engineering

PAPER • **OPEN ACCESS**

X-ray fluorescent (XRF) configuration for the measurement of mass attenuation coefficients at low energy photons

To cite this article: S N A Abdullah *et al* 2019 *IOP Conf. Ser.: Mater. Sci. Eng.* **555** 012030

IOP Conf. Series: Materials Science and Engineering **555** (2019) 012030 doi:10.1088/1757-899X/555/1/012030

X-ray fluorescent (XRF) configuration for the measurement of mass attenuation coefficients at low energy photons

Abdullah S N A[1,a)], Mohd Yusof M F[2], Kabir N A[1], Tajuddin A A[1] and Mohd Rodin M N M[1]

[1]School of Physics, Universiti Sains Malaysia, 11800 USM, Penang, Malaysia
[2] School of Health Sciences, Universiti Sains Malaysia, 16150 Kota Bharu, Kelantan, Malaysia

[a]sitinor_azizah87@yahoo.com

Abstract. An X-ray fluorescent (XRF) configuration was used to measure the mass attenuation coefficient of materials at low energy photons. An Americium-241 (^{241}Am) annular source was used in conjunction with niobium, palladium, molybdenum and tin plates that provided $K_{\alpha 1}$ photons with energies between 16.59 and 25.26 keV. The transmitted photons were measured by using a low energy Germanium (LEGe) detector and analyzed by using MAESTRO software. A calibration with ^{241}Am showed good linearity between photon energies and peak channels with R^2 value near to 1. The measurement of mass attenuation coefficient was carried out on Al plates and Perspex based on the transmitted photons on the samples. The measured mass attenuation coefficients were compared to the XCOM calculations. The results showed that the measured mass attenuation coefficients of aluminum and Perspex® were in good agreement to their XCOM values within 10% percentage of discrepancies at all experimented photon energies. The overall results indicated the suitability of the XRF configuration for the measurement of mass attenuation coefficients at low energy photons.

1. Introduction

The accurate measures of radiation interaction parameters with matter plays a significant value in many applied fields of sciences. The essential parameter, for example the attenuation coefficient of a material is extensively evaluated in medical, nuclear and radiation physics, radiation protection and dosimetry, as well as industrial, environmental and agricultural studies [1].

The probability of photon interaction by a physical process or another per unit distance travelled is called linear attenuation coefficient, μ [2]. However, mass attenuation coefficient (μ/ρ) is more important in characterization of a material. This is because it offers the reduction of photon intensity as a function of mass instead of path length of the travelled material [3]. Besides, attenuation of γ-rays and X-rays is closely related to density and atomic number of a material. Thus, it provides many other photon interaction parameters such as atomic cross-section, effective atomic number and electron density. [4]

Theoretically, XCOM computer program is commonly used for obtaining the attenuation coefficient values that can be compared experimentally [5]. However, the XCOM has a few limitations such as it does not consider the molecular and solid-state effects which can change the element's cross section. Therefore, several measurements have been reported on the experimental determination of attenuation coefficients. Some of these are using proton-induced X-ray emission (PIXE) [6], high energy gamma photon [7][8] and X-ray fluorescent (XRF) techniques [9][10].

X-ray fluorescence (XRF) spectrometry is widely used for quantitative analysis because it is inexpensive and requires less technical effort to run the system [11]. It is a non-destructive analytical technique used to determine the elemental composition of a sample by measuring the fluorescent (or secondary) X-ray emitted from the sample when it is excited by a primary radiation source. This characteristic X-ray is unique and usually defined as the fingerprint for the specific element.

This study was conducted to measure the mass attenuation coefficients of two materials: aluminum (Al) and Perspex® using XRF configuration at effective energy range of 16.59 keV to 25.26 keV. The values were then compared to the mass attenuation coefficients calculated from XCOM simulation software.

2. Materials and methods

2.1. Materials Used

Pure aluminum and Perspex® plates were used as the absorber in this experiment as shown in Figure 1. The dimension of aluminum plates are 7.6 cm x 7 cm and four thicknesses of 0.06 cm, 0.125 cm, 0.15 cm and 0.2 cm with the density of 2.70 g/cm^3. The Perspex®, with the density of 1.18 g/cm^3 has 5 cm x 5 cm dimension with thicknesses of 0.5 cm, 1 cm, 1.5 cm and 2 cm.

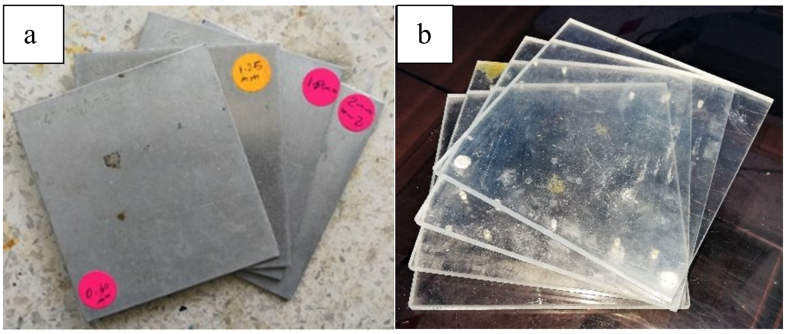

Figure 1. a) Aluminum plates and b) Perspex® used in the study.

2.2. Determination of mass attenuation coefficient using ^{241}Am source

The XRF instrument at Biophysics Laboratory, School of Physics, Universiti Sains Malaysia (USM) was used for the measurements of mass attenuation coefficient of the absorbers. A schematic drawing of the experimental arrangement is presented in Figure 2. A 59.54 keV of 100 mCi ^{241}Am was used to irradiate high purity metal plates to produce the X-ray fluorescence photons. The photons transmitted through the absorber were detected in a narrow beam geometry by the CANBERRA low energy Germanium (LEGe) detector. The detector output pulses were amplified by an ORTEC 572 amplifier and the spectrum was collected by a multichannel analyser (MCA-3 series) for a period of 60 seconds.

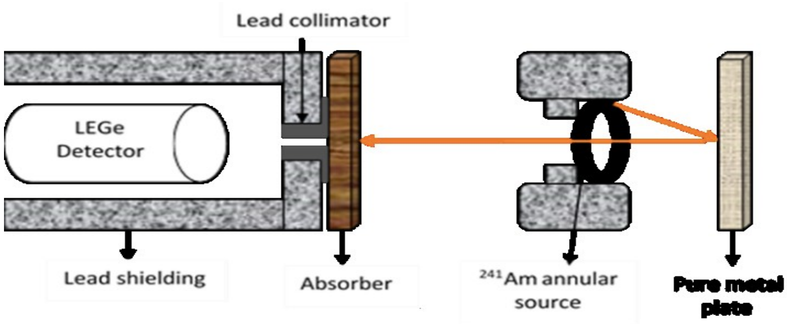

Figure 2. The schematic diagram of the experimental set-up for attenuation measurement.

In this experiment, 4 types of high purity metal plates were used: niobium (Nb), molybdenum (Mo), palladium (Pd) and tin (Sn) having $K_{\alpha1}$ fluorescent X-rays of 16.59, 17.74, 21.21 and 25.26 keV respectively. Table 1 presents the details of the metal plates [12].

Table 1. The details of metal plates used in the X-ray fluorescent (XRF) configuration.

Plate	Atomic Number (Z)	Thickness (mm)	Purity (%)	$K_{\alpha1}$ energy (keV)
Niobium (Nb)	41	0.14	99.8	16.61
Molybdenum (Mo)	42	0.11	99.9	17.47
Palladium (Pd)	46	0.10	99.9	21.17
Tin (Sn)	50	0.28	99.999	25.27

Next, the net area under the $K\alpha_1$ peak was measured, the total intensity of incident photons (N_o) and those that are transmitted without interaction (N) were calculated in unit of counts. From that, linear attenuation coefficient (μ) expressed in cm^{-1} can be calculated by

$$\mu = \frac{1}{x}\ln \frac{N_0}{N} \tag{1}$$

with x is the thickness of the absorber [13]. However, since a range of thicknesses were used, the linear attenuation coefficient was determined by the gradient of ln [N_o/N] against thickness curve.

Yet, the probability of interaction is proportional to the number of atoms per volume. This dependency can be overcome by normalizing the linear attenuation coefficient to the density of the material, defined as mass attenuation coefficient, μ/ρ (cm^2/g). After the mass attenuation coefficient of the two types of absorbers were calculated experimentally, the results were then compared to the theoretical values obtained from XCOM simulation software.

2.3. Evaluation of Statistical Analysis Using Paired Sample t-test

The paired sample *t*-test was carried out to compare the means between two sets of data and show how significant the difference was from each other. The two tailed paired-sample *t*-test was chosen for this study to prove the similarity of the mass attenuation coefficients of the absorbers obtained by XRF method and XCOM computer program. The null hypothesis was the mean difference of the mass attenuation coefficient between both methods is equal to zero, H_0: $\mu_d = 0$ [14]. In brief, the *p*-value obtained must be higher than 0.05 (5%) to show that the mass attenuation coefficients from both methods were considered statistically equivalent.

3. Results and discussion

3.1. Mass attenuation coefficient for Aluminium and Perspex® using XRF method and XCOM

The mass attenuation coefficients of Aluminium samples were determined and presented in Figure 3. The graphs showed that the values of mass attenuation coefficients decreased when the photon energies increased [1,2]. The comparison between the experimental values using XRF system and calculated values from XCOM software. Accordingly, it was found that the mass attenuation coefficient values measured using the XRF configuration were very close to the theoretical values calculated in XCOM computer program [5]. The reasonable agreement between the two measurements gave confidence in the technique adopted during the experiment.

Similar results were also observed in Perspex® as shown in Figure 4. The XCOM values of Perspex® were obtained by inserting the percentage of elemental compositions of Perspex® into the XCOM calculation software. The values of measured mass attenuation coefficients of Perspex® however showed larger differences to its respective values in XCOM at higher photon energies compared to that in the lower photon energies.

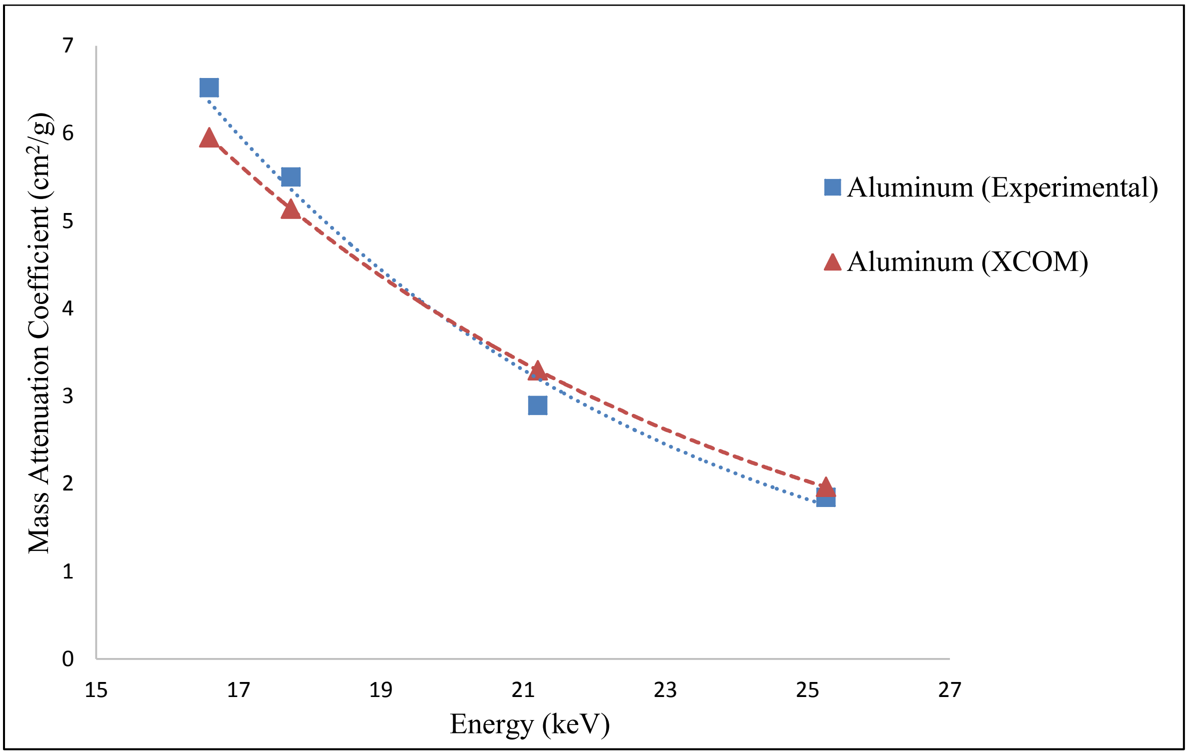

Figure 3. Mass attenuation coefficients of aluminium determined by XRF method and XCOM against photon energy.

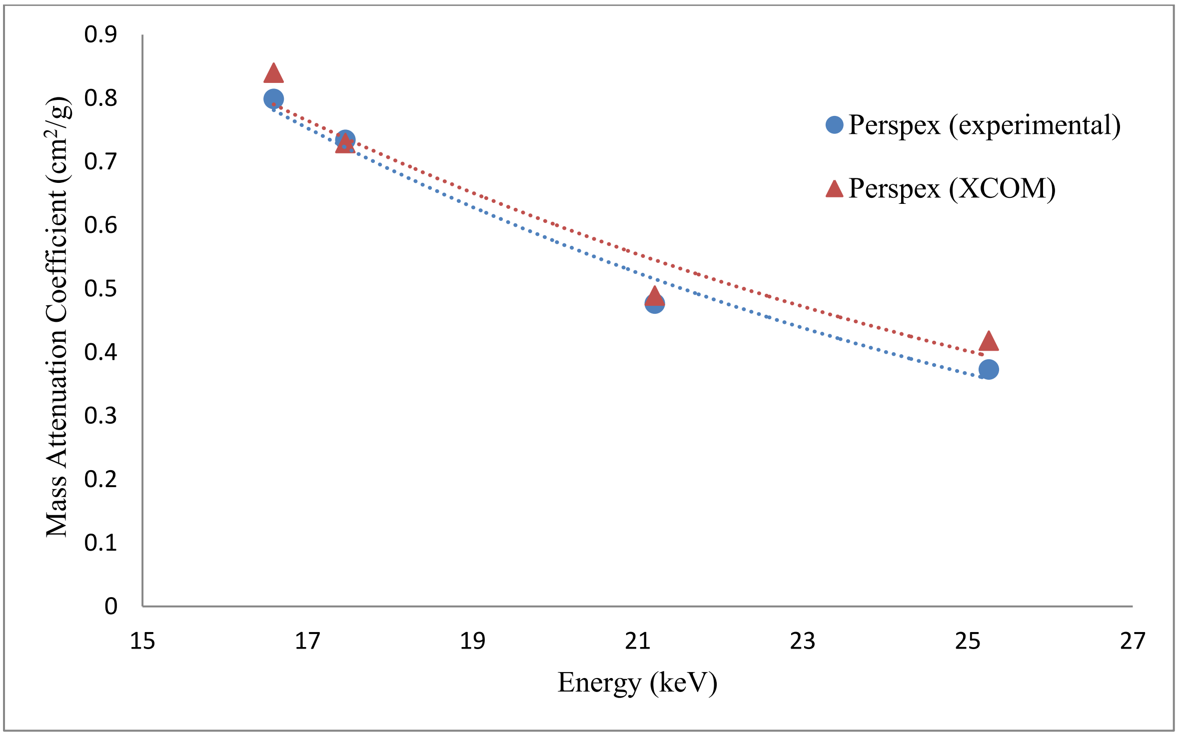

Figure 4. Mass attenuation coefficients of Perspex® determined by XRF method and XCOM against photon energy.

3.2. Paired-sample t-test analysis for mass attenuation coefficient of Aluminium and Perspex

Table 2 presented the results of the two tailed paired-sample *t*-test of mass attenuation coefficient of aluminium and Perspex®. The *p*-value for both absorbers calculated were higher than 0.05, indicating that the pairs of mass attenuation coefficient between the two methods had no significant difference. Thus, the null hypothesis was accepted. This showed the similarity between mass attenuation coefficient obtained by experiment and calculated by XCOM. Consequently, the XRF technique used in this study produced an accurate and reliable results for mass attenuation coefficient measurement.

Table 2. The paired-sample *t*-test of mass attenuation coefficients of the absorbers between experimental and XCOM values.

Pair	Paired Differences		df	t	*p*-value (two-tailed)
	Means	Standard Deviation			
Aluminum XRF - XCOM	0.102	0.385	4	0.462	0.676
Perspex XRF - XCOM	0.023	0.005	4	1.953	0.146

4. Conclusions

The comparison of the mass attenuation coefficient for both absorbers: aluminium and Perspex® showed that our experimental results were, in general, close to the theoretical values calculated using XCOM, represented by the solid curve. Furthermore, the paired-sample *t*-test indicated that the mass attenuation coefficients obtained by both methods were considered statistically equivalent. Hence, the XRF configuration in our biophysics lab is suitable and reliable to be used for mass attenuation coefficient measurement at low energy range.

5. References

[1] Marashdeh M W, Al-Hamarneh I F, Munem E M A, Tajuddin A A, Ariffin A and Al-Omari S 2015 Determining the mass attenuation coefficient, effective atomic number, and electron density of raw wood and binderless particleboards of *Rhizophora* spp. by using Monte Carlo simulation. *Results in Phys.* **5** p 228-234.

[2] Tekin H O and Manici T 2017 Simulations of mass attenuation coefficients for shielding materials using the MCNP-X code *Nucl. Sci. T*ech. **28(7)** p 95.

[3] Tousi E T, Hashim R, Bauk S and Jaafar M S 2017 Evaluation of the mass attenuation coefficient and Effective Atomic Number of the *Eremurus* spp. root in mammography energy range *IOSR-JOP* **09(01)** p 100-104.

[4] Levet A and Özdemir Y 2017 Determination of effective atomic numbers, effective electrons numbers, total atomic cross-sections and buildup factor of some compounds for different radiation sources *Radiat. Phys. Chem*. **130** p 171-176.

[5] Berger M J and Hubbell J H 1987 XCOM: Photon cross-sections on a personal computer *NBSIR* **87** p 3597.

[6] Abdullah K K, Ramachandran K K, Karunakaran N, Babu B R S, Josephm A, Thomas R and Varier K M 2010 X-ray attenuation around K-edge of Zr, Nb, Mo and Pd: A comparative study using proton-induced X-ray emission and ^{241}Am gamma rays. *Pramana J. of Phys*, **75(3)** p 459-469.

[7] Yusof M F M, Abd Hamid P N K, Tajuddin A A, Hashim R, Bauk S, Mohd Isa N. and Md Isa M. J 2017 Characterization and attenuation study on tannin-added *Rhizophora* spp. particleboard at high energy photon and electron *IOP Conf. Series: J. of Phys.* **851** p 012036.

[8] Yusof M F M, Abdullah A, Tajuddin A A, Hashim R, Bauk S 2016 Attenuation properties and percentage depth dose of tannin-based *Rhizophora* spp. particleboard phantoms using computed tomography (CT) and treatment planning system (TPS) at high energy x-ray beams *AIP Conf. Series* **1704** p 040003.

[9] Marashdeh M W, Bauk S, Tajuddin A A, and Hashim R 2012 Measurement of mass attenuation coefficients of *Rhizophora* spp. binderless particleboards in the 16.59–25.26 keV photon energy range and their density profile using x-ray computed tomography *Appl. Radiat. Isot.* **70** p 656–662.

[10] Alshipli M and Kabir N A 2017 Measurement of attenuation coefficients and CT numbers of epoxy resin and epoxy-based Rhizophora spp particleboards in computed tomography energy range. *Radiat. Phys. Chem.* **149** p 41-48.

[11] Kacal M R, Han I and Akman F 2015 Determination of K shell absorption jump factors and jump ratios of 3d transition metals by measuring K shell fluorescence parameters *Appl. Radiat. Isot.* **95** P 193-199.

[12] Yusof M F M, Abd Hamid P N K, Tajuddin A A, Hashim R and Bauk S 2015 Mass attenuation coefficient of binderless, pre-treated and tannin-based *Rhizophora* spp. particleboards using 16.59 – 25.26 keV photon energy range *AIP Conf. Series* **1659** p 040007.

[13] Bushberg J T *et al.* 2012 *The essential physics of medical imaging* (Philadelphia: Lippincott Williams & Wilkins).

[14] Abd Hamid P N K, Mohd Yusof M F, Tajuddin A A and Hashim R 2017 Measurement of mass attenuation coefficients for corn starch bonded *Rhizophora* spp. particleboards at 16-59-25.26 keV photons using X-ray fluorescence configuration *Jurnal Sains Nuklear Malaysia*, **29(2)** p 47-54.

Acknowledgements

The authors would like to thank the financial support of Incentive Grant no. 1001/PFIZIK/823048 and Bridging Grant no. 304/PPSK/6316145 by Universiti Sains Malaysia.